Design and Realization of a Sputter Deposition System for the *in situ* and *in operando* Use in Polarized Neutron Reflectometry Experiments: Novel Capabilities

Jingfan Ye[a,*], Alexander Book[a], Sina Mayr[a,1], Henrik Gabold[a], Fankai Meng[a], Helena Schäfferer[a], Ryan Need[b], Dustin Gilbert[c], Thomas Saerbeck[d], Jochen Stahn[e], Peter Böni[a], Wolfgang Kreuzpaintner[a,f,g]

[a] *Technische Universität München, Physik-Department E21, James-Franck-Str. 1, 85748 Garching, Germany*
[b] *NIST Center for Neutron Research, National Institute of Standards and Technology, Gaithersburg, Maryland 20899, USA*
[c] *Materials Science and Engineering, University of Tennessee, Knoxville, TN 37996, USA*
[d] *Institut Laue-Langevin, CS 20156, 38042 Grenoble Cedex 9, France*
[e] *Paul Scherrer Institut, 5232 Villigen PSI, Switzerland*
[f] *Institute of High Energy Physics, Chinese Academy of Sciences (CAS), Beijing 100049, China*
[g] *Spallation Neutron Source Science Center, No. 1, Zhongziyuan Road, Dalang, Dongguan 523803, China*

Abstract

Recently, the design and realization of a sputter-deposition system for *in situ* and *in operando* polarized neutron reflectometry (PNR) was reported. The device allows magnetic thin films and heterostructures to be grown, while the sample remains aligned in the neutron beam for PNR. By now, it has been applied in experiments that investigated the magnetic and structural properties of thin Fe and Pd/Fe/Pd heterostructures as a function of the layer thickness. Here, we report on significant upgrades of the deposition system with advanced thin film growth and measurement capabilities. These include improvements to the generation of the vacuum to realize ultra-high-vacuum (UHV) conditions. A base pressure below 5×10^{-9} mbar can now be obtained within less than one day of pumping time. To allow experiments over a wide range of temperatures, the system was upgraded to include a cryo-furnace. It allows the sample to be

*Corresponding author: jingfan.ye@frm2.tum.de
[1] Present address: Paul Scherrer Institut, 5232 Villigen PSI, Switzerland

cooled or heated in the range of 10 K to 1000 K for both applications, sample growth and measurement. Further, a new magnetic coil setup with soft iron yoke was designed which can realize a homogeneous in-plane magnetic field of up to 300 mT and electric fields at the sample position.

Keywords: Thin films; Neutron reflectometry; Magnetism; Instrument; Sputtering; Film deposition

1. Introduction

Since the discovery of the giant magnetoresistance (GMR) effect [1, 2], magnetic thin film heterostructures have conquered an indispensable realm in combining electronic and magnetic properties. Especially in recent years, novel approaches have been followed to couple the magnetic and electronic properties of thin films for realizing advanced functionality in spintronic devices [3, 4]. During its growth, the microstructure and morphology of a thin film, its stoichiometry and potential magnetic properties are defined. Dramatic changes typically occur at interfaces from one material to another and during the deposition of the first few layers [5, 6]. We have reported on the realization of a sputter deposition system for *in situ* and *in operando* polarized neutron reflectometry (PNR) experiments, which enables the growth of thin films while the sample remains aligned in the neutron beam [7]. In contrast to previous reports on *in situ* or quasi *in situ* PNR facilities [8–10], it is the first deposition setup which allows not only *in situ*, but also *in operando* polarized neutron reflectometry (*in operando* PNR) measurements to be performed.

The general design of our system described in [7] incorporates a sputter deposition chamber. It initially only provided the basic requirements for the deposition processes and PNR measurements and is designed as a mobile sample environment for various neutron beamlines. After initial proof-of-principle and feasibility tests, first scientific results have been obtained, e.g. on the topological and magnetic structure of epitaxially layer-by-layer grown Fe [11, 12] and the coexistence of proximity effect and Dzyaloshinskii-Moriya Interaction at the

interface of Pd/Fe [13]. The experiments demonstrated the reliability and power of *in situ* PNR by, (i) confirming most of the known thickness-dependent magnetic properties of thin Fe layers, and (ii) by uncovering unique characteristics that were previously not observed.

While the *in situ* PNR setup described in [7] is well suited for the investigation of magnetic thin films at room temperature, the investigation of novel materials and material combinations requires an improved sample environment. In particular, the ability to reach not only high, but also low temperatures is fundamental for the study of many magnetic systems. Also the application of a variable magnetic field at the sample position during both deposition and PNR measurements is essential. As an example, thin films of oxides, such as $Pb(Zr, Ti)O_3$, MgO or $BaTiO_3$ need to be grown and annealed at high temperatures of up to 1000 K in order to achieve their desired epitaxial morphology [14–17]. Most of their interesting magnetic and electromagnetic properties, however, emerge only significantly below room temperature and under application of magnetic fields. Prime examples thereof are the ferromagnetic phase of EuO [18] or the skyrmion lattice phase of FeGe [19].

Here, we report on upgrades of the *in situ* PNR chamber [7] which realizes these capabilities. The main upgrades focus on the internal sample stage. During the course of the upgrade, the vacuum system of the chamber was also improved to ultra-high-vacuum (UHV) conditions. The low base pressure of $< 5 \times 10^{-9}$ mbar now allows highly reactive materials like Dy or Eu [20, 21] to be grown *in situ*. UHV is also essential to prevent thin films of nearly any material from contamination by residual vacuum gas species during the PNR data acquisition, in particular if the sample is at very low temperatures at which sticking coefficients approach unity.

One of the most limiting parameters for any upgrade of the deposition chamber is its maximum allowed size, which is defined by the space available at a neutron beamline. Although the deposition system was originally designed for the beamline REFSANS at MLZ, Garching, Germany, it is now mainly used at the AMOR beamline at PSI, Villigen, Switzerland, for two main reasons:

(i) AMOR is more open than REFSANS, allowing the installation of a larger and more protruding sample environment and (ii) the use of the Selene guide demonstrator [11, 22] with its focused beam allowed for footprint control without diaphragms within the vacuum chamber and it provided a flux gain on the sample of a factor 4 with respect to the conventional TOF mode [23]. Along with these upgrades, the layout of the chamber and the control software were optimized on the basis of experiences gained from operation.

In the following, the implementation of a cryo-furnace (section 2), the upgrades to the vacuum system (section 3), improvements of the internal magnetic field system (section 4), the control software (section 5) as well as further minor technical improvements (section 6) will be described. In section 7, exemplary experiments are described that use these novel capabilities.

2. Cryo-furnace

The ability to cool and heat the sample while it stays aligned in the neutron beam for *in situ* PNR is realized by a cryo-furnace, which is built up of a ^{4}He-closed cycle cryostat with an integrated heater. This required a full re-design of the sample holder and the expansion of the main vacuum chamber by an attached dedicated cryostat chamber section. Special attention was also paid to the UHV compatibility of all parts inside the additional vacuum chamber.

A CAD drawing of the cryostat vacuum chamber extension, attached to the main deposition chamber, is shown in figure 1. A photograph of the full setup as installed at the AMOR beamline is shown in figure 2. The vacuum chamber of the cryostat is designed to optimize the heat transfer from the sample holder inside the UHV deposition chamber to the cold head of the cryostat. It was custom designed in collaboration with ColdEdge Technologies[2]. It is made from a DN160CF stainless steel cross and a DN160CF tube extending it to the top. The cold head (Sumitomo RDK-408D2) is installed in a receptacle, which

[2]905 Harrison Street, Allentown PA 18103 USA

is recessed into the DN160CF tube and cooled by a compressor (Sumitomo F70H). To suppress the transfer of unavoidable vibrations, the cold head and the receptacle are separated by a $\approx 5\,\mu m$ wide gap, which in turn is thermally bridged by flushing it with ^{4}He gas.

The sample holder made from gold-plated copper is in direct thermal contact with the receptacle via the cold finger. In order to minimize the intake of heat radiation, a gold-coated cold shield between the vacuum chamber and the cold rod is implemented along the full length of the cooling line. The movability of the sample holder and the capability to align it in the neutron beam is realized via a support rod, to which the sample holder is attached via a heat insulating and UHV-compatible PEEK connector. On its other end, the support rod is mounted on a DN100CF flange, which can be moved by the sample alignment stage described in [7]. Its design was not changed during the upgrade. It still allows exact movements in vertical (z) and horizontal (x) direction as well as rotations (θ) with position encoders installed on the θ and z axis as described in [7]. As novel additional alignment component, a single axis port aligner is integrated to compensate any bending of the rod for the sample holder. Both the cold shield and the support rod are cooled to $\approx 40\,K$ by the cold head's high temperature cooling stage, thus reducing the temperature difference between the cold parts and the shielding for realizing the minimum temperature of $10\,K$ at the sample holder.

A photograph of the sample holder and its surrounding is shown on the right hand side of figure 1. For heating, a heater cartridge HTR-25-100 from Lake Shore Cryotronics® is used. A sapphire heat coupling interface is installed between the sample holder and the connection to the cold finger. Sapphire is a good thermal conductor at low temperatures, but an excellent thermal insulator at elevated temperatures. As such, it forwards the cooling capacity of the cryostat directly to the sample holder at room temperature or below, but very efficiently blocks the heat from the heater cartridge to be transferred onto the cold rod at high temperatures. This allows the heating power of the heater cartridge to be concentrated onto the sample holder while the cryostat is protected

from exposure to potentially harmfully elevated temperatures. The cold shield extends beyond the heat coupling interface. The heater cartridge as well as two temperature sensors, one Pt-100 and one DT-670B-SD are installed under the copper cover of the heat coupling interface. In addition, a K-type thermocouple sensor is mounted directly underneath the sample holder and another next to the connection to the cold finger. In total, they are used for controlling the temperature of the sample holder in the temperature range $10\,\mathrm{K} \leq T \leq 1000\,\mathrm{K}$. The heater and all temperature sensors are controlled by a Lakeshore 336 temperature controller.

The cryostat is connected to the main chamber via one of the DN160CF flanges, realizing a combined vacuum regime. The cryostat ensemble is supported by a movable frame and a support made from aluminium profiles[3]. It can be lifted by up to 0.9 m to compensate any height difference of the ground levels of cryostat and sputter deposition chamber. This is of particular relevance as at the AMOR beamline, the vacuum system is positioned on the optical bench of the beamline, while the cryostat chamber rests on the lower lying main floor level next to the optical bench.

3. UHV compatibility

The base pressure of the deposition chamber in its first development phase was 1×10^{-6} mbar. The aim of improving the vacuum quality to a base pressure of $< 5 \times 10^{-9}$ mbar is to rule out any relevant surface contamination of a freshly deposited thin film by residual gas for the duration of a PNR measurement. The following approaches were taken to improve the vacuum quality:

(i) The pumping concept of the chamber was fully revised: The main turbomolecular pump (Pfeiffer Vacuum TMP 200, 200 l/s) was replaced by an Edwards STP-iX455 with a throughput of 300 l/s. Further, an ion pump (Hositrad, 100 l/s) and a Ti-sublimation pump with LN_2 cold trap were installed

[3] Minitec®

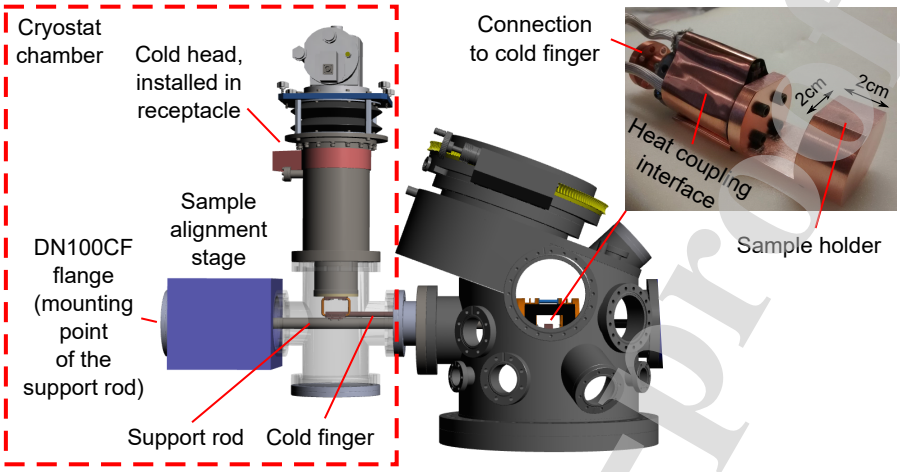

Figure 1: CAD drawing of the cryo-furnace when attached to the main deposition chamber. A photo of the disassembled sample holder including the heat coupling interface is shown on the right hand side.

for binding water and pumping lighter gas species (e.g. H_2), which cannot be pumped efficiently by pumps whose working principle is based on momentum transfer. Finally, an additional turbomolecular pump (Pfeiffer Vacuum HiPace Set 300 M, 300 l/s) with low vibrations was installed below the cryostat (figure 2).

(ii) All materials used inside the vacuum were re-evaluated for their UHV compatibility. All materials specified for only high-vacuum (HV) were replaced. This especially concerns the use of printed circuit boards and soldered electronics (internal slit system) as well as any polymer-based wire insulation. Also the internal pair of Helmholtz-coils, described in [7], was removed as it showed a higher outgassing rate than expected.

(iii) Although the vacuum chamber was originally not designed for a bake-out, an internal heating concept based on halogen lamps as heating elements was realized. In total, four heating cartridges with a heating power of 200 W each are installed on sockets on a bottom plate inside the main chamber (figure 4c). It aids in pumping the molecules with a low vapour pressure and desorption

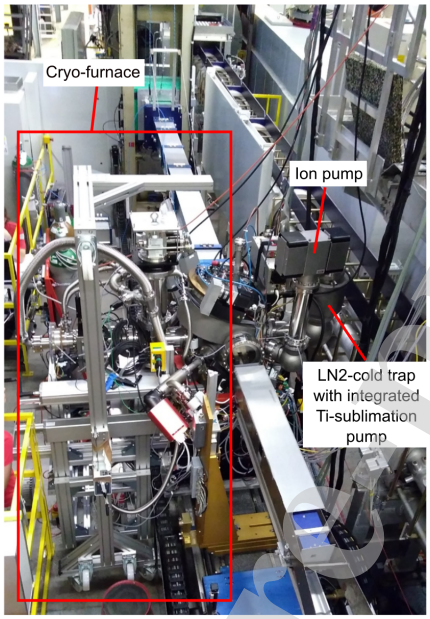

Figure 2: The *in situ* PNR sputter deposition system with attached cryo-furnace ensemble, mounted at the AMOR beamline at PSI. The newly implemented additional pumping components, consisting of an ion pump and a Ti-sublimation pump with an integrated LN_2 cold trap can also be seen.

rate (mainly water molecules).

In their combination, these measures allow a lower base pressure in a much shorter pumping time to be reached: A pressure of 1×10^{-7} mbar is achieved within 2 hours, a base pressure of 5×10^{-9} mbar within 1 day.

4. Magnetic field

As the geometry of the in-vacuum sample environment changed significantly due to the implementation of the cryo-furnace, the previously used guide fields and method to magnetize the sample needed to be adapted. In a first modification step, the Helmholtz coils of the original setup were omitted and replaced by NdFeB permanent magnets near the sample holder (figure 3). Depending on the permanent magnets used, homogeneous in-plane magnetic fields of up to 300 mT

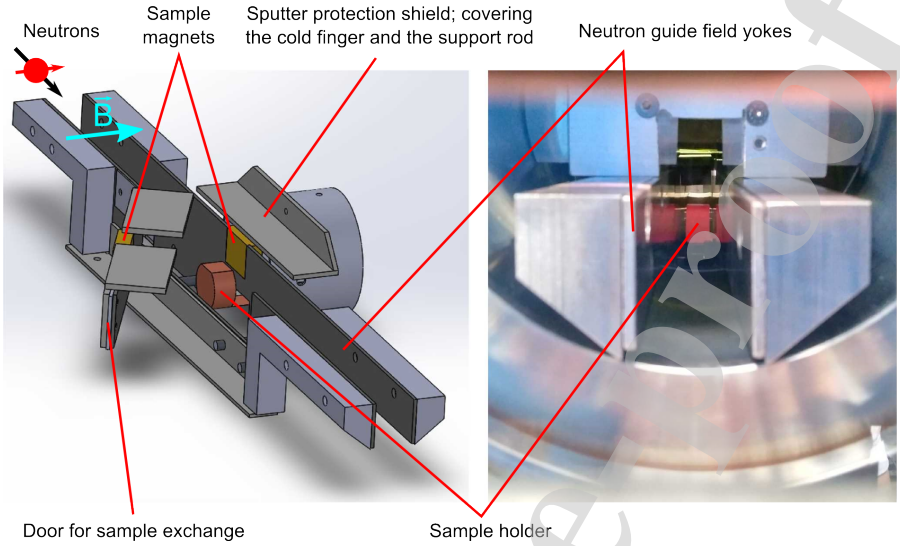

Figure 3: CAD drawing (left) and photograph (right) of the magnetic field system that is based on permanent magnets. $\vec{B}$ indicates the direction of the guide field. The connection of the sample holder to the cold finger and support rod is hidden from view by the sputter protection shield.

across the sample can be reached. For many scientific systems of interest, this field is sufficient to saturate the sample magnetically for PNR measurements. The sample magnets are part of the guide field yokes, which, before and after the sample position, generate a guide field of around 1 mT perpendicular to the scattering plane. As a consequence of the modified magnetic system, the deposition shutter also needed to be modified to account for the changed spatial boundary conditions. It is made from a 0.5 mm aluminium plate with an aperture and situated above the sample. In the closed position, the aluminium plate blocks the line of sight from the sputter gun to the sample. For sputter deposition, the shutter is rotated horizontally above the sample position until the aperture restores the direct line of sight. For finishing the deposition procedure, the shutter is rotated further until the line of sight is blocked again. Newly implemented shields protect the cold finger with the temperature sensors from pollution by any sputtered material.

Although permanent magnets can provide a 10× higher magnetic field than the Helmholtz coils of the original setup, its major drawback is that the field strength cannot be varied during the course of the measurements and deposition processes until the sample is changed. In order to further improve experimental capabilities and to allow the magnetic profiles of thin films at various magnetic fields to be investigated, a novel coil-based vectorial magnetic system with a soft-iron core, which is cooled by water, was developed and will replace the permanent-magnets setup (figure 4b). Finite element simulations using COMSOL Multiphysics® predict a homogeneous field of more than 300 mT to be reachable at the sample position. Permanent magnets along the neutron flight path provide the neutron guide field. As special feature, the yokes of the realized magnet setup can also be used as electrodes for the application of in-plane electric fields. The magnetic system is mounted on the same bottom plate on which the heating elements are installed. The complete field system is constructed such that the cryogenic setup and capabilities described in section 2 can be maintained. To ensure a better overview, the cold finger and cooling shields are not shown here.

5. Reorganization of Chamber Control

With the upgrade of the *in situ* sputter deposition chamber, also the control hardware and software were entirely revised. Power supplies, pump and vacuum controllers, other required peripheral equipment as well as the control computer, which used multiple racks in the original setup, have now been combined into one single 19" double width rack.

The devices are still addressed by the control computer via TCP/IP, USB or RS-232. However, a new Python command library was developed, which replaces the formerly used LabView® software. It has a significantly simpler structure, is much easier to expand and communicates more reliably and faster with the beamline computers. Moreover, scripts for automating film deposition steps can now be easily written and executed with full flexibility.

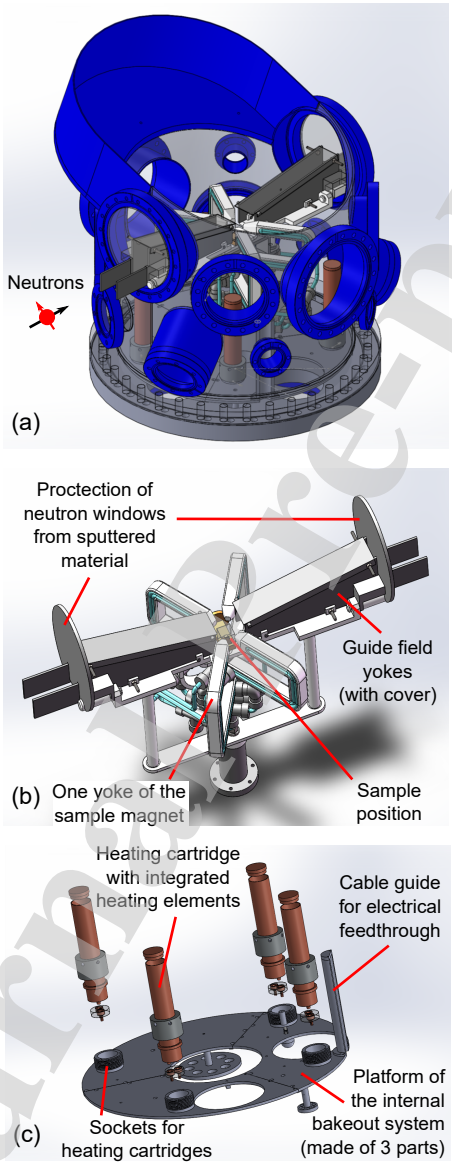

Figure 4: (a) CAD drawing of the upgraded main chamber. (b) Drawing of the magnetic coil system (wires of the coils are not shown) and (c) the upgraded heating system.

For an overview on all status parameters, a novel graphical user interface was developed, based on the PyQt library [24]. It polls and refreshes the status of important device parameters approximately once per second. For the operation of the sputter chamber at neutron beamlines, a communication server was programmed which offers an interface for external computers. This interface enables the full and direct control of the *in situ* sputter chamber by the beamline computer, in particular the sample alignment and the film deposition. The source code of all the packages and their documentation are available at `https://github.com/TUM-E21-ThinFilms` [25] under the General Public License (GNU version 3.0).

In addition to the computer control and the communication with the peripheral components, also the electrical connections and the cable management of all devices were completely revised. The main purpose was a tidier wiring that is easy to maintain and which allows a simple integration of new devices. In the new power management system, every controller device is located inside the double-width 19" rack. The rack is powered by three 16 A 3-phase CEE electricity connectors. One of them powers three 24 VDC voltage sources. A central distributor platform inside the rack acts as an electric hub for all the power sources, either 230 VAC (star-connection), 400 VAC (delta-connection) or 24 VDC. This hub distributes the power to 50 triple-deck terminal blocks, where almost all devices of the rack and the chamber are connected.

An aluminium front plate holds the most important control buttons and status indicators. On the rear side, an aluminium panel which contains feedthroughs for almost all outgoing cables of the devices inside the rack is installed. It works as a unified connection point for all cables which have to be connected to the deposition chamber.

6. Further Technical Improvements

Some additional small technical improvements of the deposition system were made:

- For the control of the gas pressure during sputter deposition, the originally used mass flow controllers [7] were replaced by leak valves (VAT 59024-GEGG) which are able to regulate the working gas pressure with an accuracy of better than 1% of any preset pressure.

- A sputter process monitor (SPM 220 by Pfeiffer Vacuum) was installed to analyze the gas composition of the residual gas of the chamber at base pressure and of the working gas during the sputter deposition process.

- For a more precise control of the sputtering power, two DC sputter power supplies (ADL GS 05 / 1000 V) with a minimum power of 2 W and a maximum power of 500 W replaced the originally implemented Trumpf TruPlasma DC 3001 power supply.

- Cooling of the sputter guns and the power supply for RF-sputtering is now realized using an air-cooled recirculating cooler (Julabo FL4003). It is independent of central cooling water supply and can regulate temperatures between $-20\,^{\circ}\mathrm{C}$ and $40\,^{\circ}\mathrm{C}$ with a precision of $0.1\,^{\circ}\mathrm{C}$. The choice of the exact temperature of the sputter deposition source is important for materials whose sputtering yields depend on the temperature of the sputter target. In particular, magnetron sputtering of ferromagnetic target materials is influenced by magnetic shielding of the sputter target. A very prominent example is Gd with a Curie temperature of $T_C \approx 19\,^{\circ}\mathrm{C}$ [26]. Here, the shielding effect can be completely suppressed if the target temperature is kept above T_C by the temperature of the cooling liquid.

7. Exemplary Experiments

The completion of the development of the *in situ* sample environment for polarized neutron reflectometry (*in situ* PNR), and of the technique as such opens the door for novel experiments and investigations. In a first example, layered oxide/ferromagnetic tunnel junctions, which play an important role in modern spintronics and whose magnetic anisotropies, spin transport, and tunnel

magnetoresistance are directly coupled to the morphology of each layer, were investigated. *In situ* PNR at different stages of growth allowed a precise determination of the influence of the layers onto each other. This more detailed knowledge of the evolution and interplay of thin film properties during the deposition, which was not accessible before in *ex situ* measurements [27–29], provides a better understanding of the physics during the fabrication and opens up the opportunity to tune sample properties to desired needs.

In another example, *in situ* PNR is used to study the time dependent evolution of the magnetic depth profile of magnetic $La_{1-x}Sr_xMnO_3$ (LSMO) thin films. The properties of magnetic oxide thin films often depend strongly on their oxygen stoichiometry [30]. Recent studies have shown that a Gd capping layer with its strong oxygen affinity is able to enforce an oxygen migration from oxide ferromagnets into the Gd capping layer over long distances (>40 nm). This process suppresses ferromagnetism and induces electronic and structural phase transitions [31, 32]. Using *in situ* deposition capabilities, a spatial and time resolved evolution the oxygen migration and its impact on the magnetization can be observed for different temperatures. The data can be used to control the oxygen distributions in metal-oxide heterostructures, which are not only designed according to their electronic and magnetic properties, but also thermal, optical and mechanical properties.

8. Summary and Outlook

The sputter deposition system for *in situ* and *in operando* experiments by means of the reflection of polarized neutrons is now fully developed and thus offering a broad range of sample conditions for the growth and *in situ* PNR analysis of a wide range of materials. Despite the restrictions imposed by the limited space available at neutron beamlines, sample temperatures in the range of 10 K to 1000 K and a variable magnetic field of up to 300 mT were realized. The yokes of the magnets can be additionally used as electrodes for the application of electric fields. The system is ultra-high-vacuum compatible with

a base pressure $< 5 \times 10^{-9}$ mbar. In combination with the drastically reduced data accumulation times achieved by using the Selene setup at AMOR [23], a sufficient cleanliness of the sample surface between the deposition steps could be maintained for all experimental cases investigated so far (e.g. [11, 13]).

On the basis of the experience gained by operating the system, many hardware components were changed or optimized. On the software side, a Python package was developed which reliably controls the system and easily interacts with the computers that are used for controlling the beamline. A renewed device and cable management allows a simple overview of the distribution of power and signal cables, facilitating both an efficient troubleshooting and a simple expansion of the system.

Together with the massively increased brilliance of the future European Spallation Source (ESS) in combination with improved neutron optical concepts, the *in situ* PNR technique may be enhanced to a *quasi in operando* mode, where individual PNR measurements can be taken within a few seconds or even below a second and the growth can be monitored without interrupting the deposition process. The upgraded *in situ* PNR sputter chamber is therefore not only useful for present *in situ* PNR experiments but pioneers the experience and knowledge for the potential implementation of the *quasi in operando* technique at ESS.

9. Acknowledgements

The work was supported by the Deutsche Forschungsgemeinschaft (DFG) Grant No. TRR 80 (project E4) and is based on experiments performed at the Swiss spallation neutron source SINQ, Paul Scherrer Institute, Villigen, Switzerland. R.N. acknowledges support from the National Research Council Research Associateship Program. Certain commercial equipment is identified in this paper to foster understanding. Such identification does not imply recommendation or endorsement by NIST, nor does it imply that the materials or equipment identified are necessarily the best available for the purpose.

References

[1] Baibich, Broto, Fert, D. F. van Nguyen, Petroff, Etienne, Creuzet, Friederich, Chazelas, Giant magnetoresistance of (001)Fe/(001)Cr magnetic superlattices, Physical review letters 61 (1988) 2472–2475. doi:10.1103/PhysRevLett.61.2472.

[2] G. Binasch, P. Grünberg, F. Saurenbach, W. Zinn, Enhanced magnetoresistance in layered magnetic structures with antiferromagnetic interlayer exchange, Physical Review B 39 (1989) 4828–4830. doi:10.1103/PhysRevB.39.4828.

[3] S. Middey, J. Chakhalian, P. Mahadevan, J. W. Freeland, A. J. Millis, D. D. Sarma, Physics of ultrathin films and heterostructures of rare-earth nickelates, Annual Review of Materials Research 46 (2016) 305–334. doi:10.1146/annurev-matsci-070115-032057.

[4] M. Gibert, M. Viret, A. Torres-Pardo, C. Piamonteze, P. Zubko, N. Jaouen, J.-M. Tonnerre, A. Mougin, J. Fowlie, S. Catalano, A. Gloter, O. Stéphan, J.-M. Triscone, Interfacial control of magnetic properties at $LaMnO_3/LaNiO_3$ interfaces, Nano letters 15 (2015) 7355–7361. doi:10.1021/acs.nanolett.5b02720.

[5] J. Giergiel, J. Kirschner, J. Landgraf, J. Shen, J. Woltersdorf, Stages of structural transformation in iron thin film growth on copper (100), Surface Science 310 (1994) 1–15. URL: http://www.sciencedirect.com/science/article/pii/003960289491365X. doi:10.1016/0039-6028(94)91365-X.

[6] L. Brey, Electronic phase separation in manganite-insulator interfaces, Physical Review B 75 (2007) 104423. URL: http://link.aps.org/pdf/10.1103/PhysRevB.75.104423. doi:10.1103/PhysRevB.75.104423.

[7] A. Schmehl, T. Mairoser, A. Herrnberger, C. Stephanos, S. Meir, B. Förg, B. Wiedemann, P. Böni, J. Mannhart, W. Kreuzpaintner, Design and

realization of a sputter deposition system for the in situ - and in operando -use in polarized neutron reflectometry experiments, Nuclear Instruments and Methods in Physics Research Section A: Accelerators, Spectrometers, Detectors and Associated Equipment 883 (2018) 170–182. doi:10.1016/j.nima.2017.11.086.

[8] T. Nawrath, H. Fritzsche, F. Klose, J. Nowikow, H. Maletta, In situ magnetometry with polarized neutrons on thin magnetic films, Physical Review B 60 (1999) 9525. URL: http://link.aps.org/pdf/10.1103/PhysRevB.60.9525. doi:10.1103/PhysRevB.60.9525.

[9] J. A. Dura, J. LaRock, A molecular beam epitaxy facility for in situ neutron scattering, Review of Scientific Instruments 80 (2009) 073906. URL: https://aip.scitation.org/doi/pdf/10.1063/1.3169506. doi:10.1063/1.3169506.

[10] A. S. Mohd, S. Pütter, S. Mattauch, A. Koutsioubas, H. Schneider, A. Weber, T. Brückel, A versatile uhv transport and measurement chamber for neutron reflectometry under uhv conditions, Review of Scientific Instruments 87 (2016) 123909. URL: https://aip.scitation.org/doi/pdf/10.1063/1.4972993. doi:10.1063/1.4972993.

[11] W. Kreuzpaintner, B. Wiedemann, J. Stahn, J.-F. Moulin, S. Mayr, T. Mairoser, A. Schmehl, A. Herrnberger, P. Korelis, M. Haese, J. Ye, M. Pomm, P. Böni, J. Mannhart, In situ polarized neutron reflectometry: Epitaxial thin-film growth of fe on cu(001) by dc magnetron sputtering, Physical Review Applied 7 (2017). doi:10.1103/PhysRevApplied.7.054004.

[12] D. L. Cortie, G. L. Causer, K. C. Rule, H. Fritzsche, W. Kreuzpaintner, F. Klose, Two–dimensional magnets: Forgotten history and recent progress towards spintronic applications, Advanced Functional Materials (2019). URL: https://onlinelibrary.wiley.com/doi/full/10.1002/adfm.201901414. doi:10.1002/adfm.201901414.

[13] S. Mayr, J. Ye, J. Stahn, B. Knoblich, O. Klein, D. A. Gilbert, M. Albrecht, A. Paul, P. Böni, W. Kreuzpaintner, Indications for dzyaloshinskii-moriya interaction at the Pd/Fe interface studied by in situ polarized neutron reflectometry, Phys. Rev. B 101 (2020) 024404. URL: https://link.aps.org/doi/10.1103/PhysRevB.101.024404. doi:10.1103/PhysRevB.101.024404.

[14] P. M. Leufke, R. Kruk, Di Wang, C. Kübel, H. Hahn, Ferroelectric vs. structural properties of large-distance sputtered epitaxial LSMO/PZT heterostructures, AIP Advances 2 (2012) 032184. doi:10.1063/1.4756997.

[15] Y. Kaneko, N. Mikoshiba, Tsutomu Yamashita, Preparation of mgo thin films by rf magnetron sputtering, Japanese Journal of Applied Physics 30 (1991) 1091. URL: https://iopscience.iop.org/article/10.1143/JJAP.30.1091/pdf. doi:10.1143/JJAP.30.1091.

[16] K. Fujimoto, Y. Kobayashi, K. Kubota, Growth of batio3-srtio3 thin films by r.f. magnetron sputtering, Thin Solid Films 169 (1989) 249–256. URL: http://www.sciencedirect.com/science/article/pii/0040609089907086. doi:10.1016/0040-6090(89)90708-6.

[17] D. Cáceres, I. Colera, I. Vergara, R. González, E. Román, Characterization of mgo thin films grown by rf-sputtering, Vacuum 67 (2002) 577–581. doi:10.1016/S0042-207X(02)00251-8.

[18] S. Mühlbauer, P. Böni, R. Georgii, A. Schmehl, D. G. Schlom, J. Mannhart, Field and temperature dependence of the magnetization in ferromagnetic euo thin films, Journal of Physics: Condensed Matter 20 (2008) 104230. URL: https://iopscience.iop.org/article/10.1088/0953-8984/20/10/104230/pdf. doi:10.1088/0953-8984/20/10/104230.

[19] J. C. Gallagher, K. Y. Meng, J. T. Brangham, H. L. Wang, B. D. Esser, D. W. McComb, F. Y. Yang, Robust zero-field skyrmion formation in fege epitaxial thin films, Physical review letters 118 (2017) 027201. doi:10.1103/PhysRevLett.118.027201.

[20] G. Scheunert, W. R. Hendren, A. A. Lapicki, P. Jesudoss, R. Hardeman, M. Gubbins, R. M. Bowman, Improved magnetization in sputtered dysprosium thin films, Journal of Physics D: Applied Physics 46 (2013) 152001. URL: https://iopscience.iop.org/article/10.1088/0022-3727/46/15/152001/pdf. doi:10.1088/0022-3727/46/15/152001.

[21] J. W. Coburn, K. Lee, Sputter deposition of euo thin films, Journal of Applied Physics 42 (1971) 5903. URL: https://aip.scitation.org/doi/pdf/10.1063/1.1660048. doi:10.1063/1.1660048.

[22] J. Stahn, A. Glavic, Focusing neutron reflectometry: Implementation and experience on the tof-reflectometer amor, Nuclear Instruments and Methods in Physics Research Section A: Accelerators, Spectrometers, Detectors and Associated Equipment 821 (2016) 44–54. doi:10.1016/j.nima.2016.03.007.

[23] J. Stahn, U. Filges, T. Panzner, Focusing specular neutron reflectometry for small samples, The European Physical Journal Applied Physics 58 (2012) 11001. URL: https://www.epjap.org/articles/epjap/pdf/2012/04/ap110295.pdf. doi:10.1051/epjap/2012110295.

[24] Riverbank Computing Limited, Pyqt, 2018. URL: https://riverbankcomputing.com/software/pyqt/intro.

[25] A. Book, J. Ye, Tum-e21-thinfilms, 2019. URL: https://github.com/TUM-E21-ThinFilms.

[26] C. D. Graham, Magnetic behavior of gadolinium near the curie point, Journal of Applied Physics 36 (1965) 1135. URL: https://aip.scitation.org/doi/pdf/10.1063/1.1714135. doi:10.1063/1.1714135.

[27] S. Ikeda, K. Miura, H. Yamamoto, K. Mizunuma, H. D. Gan, M. Endo, S. Kanai, J. Hayakawa, F. Matsukura, H. Ohno, A perpendicular-anisotropy cofeb–mgo magnetic tunnel junction, Nature materials 9 (2010)

721. URL: https://www.nature.com/articles/nmat2804.pdf. doi:10.1038/nmat2804.

[28] M. Raju, S. Chaudhary, D. K. Pandya, Effect of interface on magnetic properties of $Co_{20}Fe_{60}B_{20}$ in ion-beam sputtered Si/CoFeB/MgO and Si/MgO/CoFeB bilayers, Journal of Magnetism and Magnetic Materials 332 (2013) 109–113. URL: http://www.sciencedirect.com/science/article/pii/S0304885312009961. doi:10.1016/j.jmmm.2012.12.022.

[29] I. Barsukov, Y. Fu, C. Safranski, Y.-J. Chen, B. Youngblood, A. M. Gonçalves, M. Spasova, M. Farle, J. A. Katine, C. C. Kuo, I. N. Krivorotov, Magnetic phase transitions in ta/cofeb/mgo multilayers, Applied Physics Letters 106 (2015) 192407. URL: https://aip.scitation.org/doi/pdf/10.1063/1.4921306. doi:10.1063/1.4921306.

[30] M. Huijben, L. W. Martin, Y.-H. Chu, M. B. Holcomb, P. Yu, G. Rijnders, D. H. A. Blank, R. Ramesh, Critical thickness and orbital ordering in ultrathin $La_{0.7}Sr_{0.3}MnO_3$ films, Physical Review B 78 (2008) 094413. URL: http://link.aps.org/pdf/10.1103/PhysRevB.78.094413. doi:10.1103/PhysRevB.78.094413.

[31] A. J. Grutter, D. A. Gilbert, U. S. Alaan, E. Arenholz, B. B. Maranville, J. A. Borchers, Y. Suzuki, K. Liu, B. J. Kirby, Reversible control of magnetism in $La_{0.67}Sr_{0.33}MnO_3$ through chemically-induced oxygen migration, Applied Physics Letters 108 (2016) 082405. URL: https://aip.scitation.org/doi/pdf/10.1063/1.4942645. doi:10.1063/1.4942645.

[32] D. A. Gilbert, A. J. Grutter, P. D. Murray, R. V. Chopdekar, A. M. Kane, A. L. Ionin, M. S. Lee, S. R. Spurgeon, B. J. Kirby, B. B. Maranville, A. T. N'Diaye, A. Mehta, E. Arenholz, K. Liu, Y. Takamura, J. A. Borchers, Ionic tuning of cobaltites at the nanoscale, Physical Review Materials 2 (2018) 2. doi:10.1103/PhysRevMaterials.2.104402.

Declaration of interests

☒ The authors declare that they have no known competing financial interests or personal relationships that could have appeared to influence the work reported in this paper.

☐The authors declare the following financial interests/personal relationships which may be considered as potential competing interests:

CRediT author statement

Jingfan Ye: Conceptualization, Methodology, Software, Validation, Investigation, Resources, Writing - Original Draft, Writing - Review & Editing, Visualization, Project administration

Alexander Book: Conceptualization, Methodology, Software, Validation, Investigation, Resources, Visualization, Writing - Review & Editing, Project administration

Sina Mayr: Validation, Investigation, Resources, Visualization, Writing - Review & Editing

Henrik Gabold: Validation, Investigation, Resources, Visualization

Fankai Meng: Resources

Helena Schäfferer: Resources

Ryan Need: Conceptualization, Resources

Dustin Gilbert: Conceptualization, Resources

Thomas Saerbeck: Conceptualization

Jochen Stahn: Conceptualization, Resources

Peter Böni: Conceptualization, Methodology, Writing - Review & Editing, Project administration, Supervision, Funding acquisition

Wolfgang Kreuzpaintner: Conceptualization, Methodology, Validation, Investigation, Resources, Writing - Review & Editing, Visualization, Project administration, Supervision, Funding acquisition